ADVANCED MATERIALS INTERFACES
Open Access
www.advmatinterfaces.de

From Surfactants to Viscoelastic Capsules

*Gaia De Angelis, Natascha Gray, Viviane Lutz-Bueno, and Esther Amstad**

Micrometer sized capsules are often used as single entities for the encapsulation and release of active ingredients, for example in food, cosmetics, and drug delivery. Important parameters that determine the stability of capsules and the release of reagents contained in them are the dimensions and composition of their shell. Most capsule shells are rather thick, thereby occupying a significant fraction of the capsule volume, or they are rigid, making the capsules fragile. This work introduces viscoelastic capsules with very thin shells of order 10 nm. Despite the thin nature of these shells, they are flexible, self-healing, yet, for practical applications impermeable even to low molecular weight substances. These shells are formed by ionically crosslinking surfactants that are functionalized with catechol-derivatives. This work investigates the influence of the number of chelators contained per surfactant and the crosslinking ion on the rheological properties of the membranes and relate it to the mechanical properties of the resulting capsules. This work demonstrates that these shells are impermeable to molecules as small as 340 Da even if loaded with cell culture media, indicating their potential for biomedical applications.

1. Introduction

Capsules are commonly used in drug delivery,[1] food,[2] and cosmetics[3] to encapsulate active ingredients and provide them with a higher stability when exposed to adverse conditions such as elevated temperatures[4] and pH changes,[5] or to prevent undesired or premature contacts with reagents, such as oxygen[6] or other proteins present in the formulation.[7] The performance of capsules is heavily based on the ability to control the permeability of their shells, which defines the time and rate of release of encapsulants. For example, size-selectively permeable capsules are frequently used to perform cell studies.[8] For cells that are located within drops or capsules to survive for a prolonged time, these compartments must enable exchanges of nutrients and waste products. Unfortunately, cell culture media buffers that are preferentially used in most of these studies, often cause coalescence of emulsions, due to their salt contents.[9] This shortcoming can be addressed if double emulsions are used as they are less prone to coalescence if loaded with media containing high salt concentrations.[10] These double emulsions can be converted into capsules with well-defined dimensions and compositions through the solidification of their shells.[11–14] The resulting capsules typically have rather rigid shells with thicknesses ≈5 μm or above. However, the throughput at which such double emulsions with controlled dimensions can be produced is very low such that they can only be used for niche applications. This weakness can be addressed if capsules are produced through more scalable approaches. The simplest type of emulsions, single emulsions, can be fabricated at very high throughputs through bulk emulsification techniques such as via vortexing[15] or sonication,[16] yet at the expense of the size control.[17] Single emulsions with well-defined dimensions can be produced at reasonably high rates if formed with membranes,[18] or parallelized microfluidic devices.[19–21] Yet, single emulsions are most frequently converted into microparticles possessing a solid core.[22] To convert single emulsions into capsules possessing a liquid core, the solidification process must be confined to their surfaces. This confinement can be achieved, for example, by stabilizing single emulsions with functional surfactants that can be crosslinked at the drop surface. For example, surfactants containing methoxysilyl (-SiOCH$_3$),[23] epoxy,[24] or methacrylate groups[25] have been converted into capsules by covalently crosslinking them at the drop surface.[24] Unfortunately, these capsules typically have rather rigid, fragile shells that tend to break upon up concentration. More elastic, mechanically stable capsules can be formed if surfactants are reversibly crosslinked, for example through metal-ligand interactions. A nature-inspired metal-ligand pair that received a particularly high interest in synthetic soft materials is the catechol-ferric ion pair. This chelator-ion pair has been used in self-healing hydrogels,[26–30] or to render densely packed microgels electrically conductive.[31] In addition, catechol-functionalized surfactants have been used to stabilize 100 μm diameter emulsions.[32] These emulsions were converted into viscoelastic capsules through crosslinking of the surfactants localized in proximity to the capsule surface with Fe^{3+}. However, because of

G. De Angelis, N. Gray, E. Amstad
Soft Materials Laboratory
Institute of Materials
École Polytechnique Fédérale de Lausanne (EPFL)
CH-1015 Lausanne, Switzerland
E-mail: esther.amstad@epfl.ch
V. Lutz-Bueno
Laboratory for Neutron Scattering and Imaging
Paul Scherrer Institut
PSI 5232 Villigen, Switzerland

The ORCID identification number(s) for the author(s) of this article can be found under https://doi.org/10.1002/admi.202202450.

DOI: 10.1002/admi.202202450

the catechol chemistry, these capsules were only stable at pHs above 8.5, severely limiting their applicability. Moreover, these surfactants were only end-functionalized with one catechol per molecule such that they could not be converted into thin percolating films. Instead, each Fe^{3+} ion could bind to up to three surfactants, resulting in aggregates that formed rather thick, discontinuous shells whose mechanical properties and permeabilities were ill-defined. To gain a better control over these parameters and hence, over the mechanical properties of the capsules, new surfactants that can form percolating deformable, yet reversible networks at the drop surface are required.

In this paper, we introduce surfactants that are functionalized with two catechol derivatives per molecule. We demonstrate that these bifunctional surfactants can be converted into thin viscoelastic self-healing shells that are sufficiently robust to sustain centrifugation at 1000 g, or osmotic pressures of order 100 kPa. We investigate the influence of the surfactant composition on the interfacial tension and its packing density in 2D and relate these parameters to the 2D rheological properties of the membranes and the capsule shell thickness. We demonstrate that these parameters are directly linked to the stability and permeability of the capsules. To enable the use of these capsules over a wide pH range, we exchange the commonly used catechols with pyrogallols that can be ionically crosslinked with a variety of divalent and trivalent ions even under physiologic conditions.[33] We demonstrate that such capsules are impermeable to molecules as small as 340 Da, even if loaded with cell culture media and used under physiologic conditions.

2. Results and Discussion

To produce capsules with dell-defined sizes, we form water-in-oil emulsion drops with a diameter of 100 µm using microfluidic devices. We employ water containing 20 mM Fe^{3+} at pH 9 as a dispersed aqueous phase and HFE7100, a perfluorinated oil, containing 1 wt% surfactant as a continuous phase. Emulsion drops are converted into viscoelastic capsules by ionically crosslinking the surfactants located at the drop surface. Surfactants functionalized with only one chelator per molecule cannot form percolating 2D films. Instead, up to three surfactants bind to each Fe^{3+} ion resulting in distinct, small clusters, as schematically illustrated in **Figure 1**a. To convert surfactants into percolating 2D films, we functionalize them with two chelators per molecule, as schematically shown in Figure 1b. We employ a block-copolymer surfactant composed of a perfluoropolyether block (FSH) that is covalently linked to a hydrophilic block made of an aliphatic polyether diamine derived from a propylene oxide-capped polyethylene glycol (Jeffamine900, or J900) as a model surfactant. To enable ionic crosslinking, we couple two catechols to the two amines that are presented at the end of the hydrophilic block, as shown in

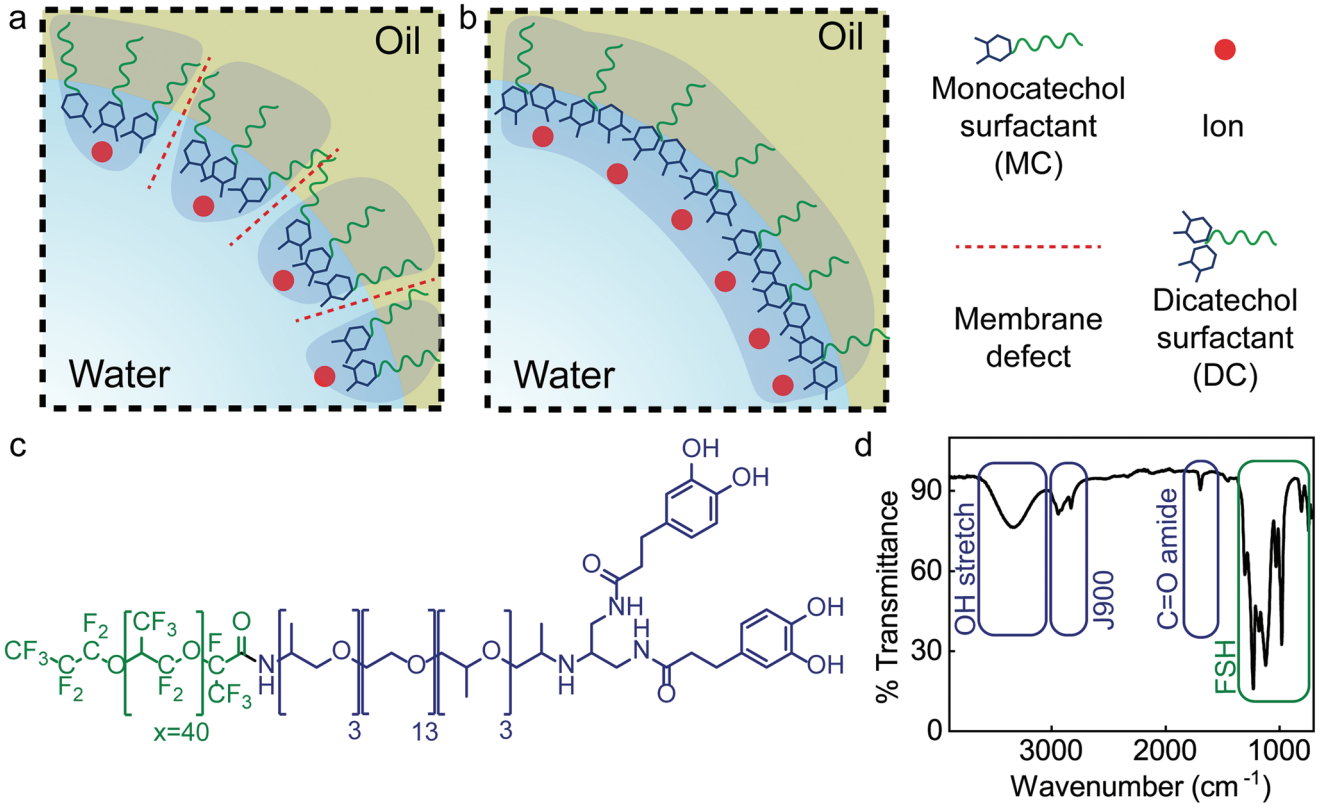

Figure 1. Schematic illustration of water-in-oil emulsions stabilized with a) monocatechol (MC) surfactants and b) dicatechol (DC) surfactants in the presence of ions that crosslink the surfactants at the drop surface. The number of defects in the membrane is drastically reduced when b) the emulsions are stabilized with dicatechol (DC) surfactants. c) Molecular structure of DC functionalized surfactant with d) the FTIR spectrum of the finished product, highlighting the characteristic peaks.

Figure 1c. Even though the small alkyl chain and the phenyl ring impart some hydrophobicity to the system, these functional groups are not fluorophilic such that if covalently linked to a hydrophilic chain, such as PEG, we expect them to be preferentially located in the aqueous phase. This expectation is supported by the fact, that ionically crosslinked capsules that are dispersed in the oil phase do not stick to each other, in stark contrast to oil-in-water drops that have been stabilized with the same surfactants. Indeed, oil-in-water drops that have been stabilized with the same surfactants present catechols at their surface such that these drops are crosslinked upon addition of appropriate ions, forming drop aggregates, as shown in Figure S1, Supporting Information. These results demonstrate that the catechol derivatives are primarily located within the aqueous phase.

To characterize our surfactants, we perform Nuclear Magnetic Resonance (NMR) spectroscopy on the first intermediate step and Fourier-transform infrared (FTIR) analysis on the entire surfactant. The successful grafting of the first step of the synthesis, the grafting of two catechols, or catechol derivatives, to 1,3-diaminopropan-2-ol, is confirmed through NMR (Figures S2–S4, Supporting Information), while the DC intermediate is confirmed through FTIR (Figure S5, Supporting Information). FTIR analysis reveals the successful functionalization of the surfactant through the characteristic peaks for the OH groups from the catechols at ≈3600 cm^{-1}, that of the J900 block at ≈2900 cm^{-1}, the C=O stretch from the amide bond at ≈1700 cm^{-1} and the characteristic FSH fingerprint between 500 and 1300 cm^{-1}, as shown in Figure 1d. Additional information on the surfactant synthesis is included in Figures S6–S9, Supporting Information.

To assess if we can convert dicatechol functionalized surfactants into viscoelastic membranes through ionic crosslinking, we perform interfacial rheology. Indeed, the storage modulus (G′) increases upon crosslinking the surfactants with 2 mM Fe^{3+} at pH 9, as shown in **Figure 2**a. Under these conditions, we reach a plateau value of the storage modulus of 0.007 N m^{-1} within 5 min. However, the membrane is rather soft. To test if we can further strengthen the membrane, we increase the Fe^{3+} concentration 10-fold to 20 mM. Indeed, these membranes are significantly stiffer, as shown in Figure 2a. Under these conditions, iron-tris agglomerates continuously precipitate at the interface, causing the storage modulus to increase over many hours in stark contrast to what we observed for membranes that have been crosslinked with 2 mM Fe^{3+} only, as shown in Figure 2b. Note that the surface to volume ratio of our capsules is ≈60 000 m^{-1}. This value is much higher than the ratio between the interfacial area in the interfacial rheology set-up and the aqueous volume present within these measurements, which is 1000 m^{-1}. Hence, we expect our capsule membranes to reach equilibrium much faster than what we observe in the interfacial rheology experiments. For this reason and because of the much stronger membranes, we will use 20 mM Fe^{3+} to crosslink our capsules for the remainder of the experiments. To prevent changes in the membrane properties of capsules over time, they can be transferred into an iron-free solution to quench the precipitation of iron-tris agglomerates.

Liquid-liquid interfaces can be rendered elastic if they are stabilized with a high density of colloids.[34] To exclude that the measured increase in storage and loss moduli is a result of surfactant-Fe^{3+} aggregates that are localized at the liquid-liquid interface, we intentionally form such aggregates using a surfactant that has been functionalized with one catechol per molecule only. The storage modulus of membranes composed of Fe^{3+}/monocatechol surfactant agglomerates is fourfold lower compared to that of the dicatechol functionalized surfactant/Fe^{3+} counterparts after 4 h, as summarized in Figure 2b. Similarly, the loss modulus (G″) of membranes formed by crosslinking Fe^{3+}/monocatechol surfactant aggregates is four times lower than that of structures formed from the dicatechol surfactant that has been crosslinked with Fe^{3+}, as shown in Figure 2b. These results suggest that difunctional surfactants can indeed be converted into a percolating network if crosslinked with Fe^{3+} at pH 9.

Chelators and Fe^{3+} interact dynamically. Hence, we expect films composed of dicatechol functionalized surfactants that are crosslinked through Fe^{3+} to be self-healing. To test this expectation, we perform strain recovery measurements by straining

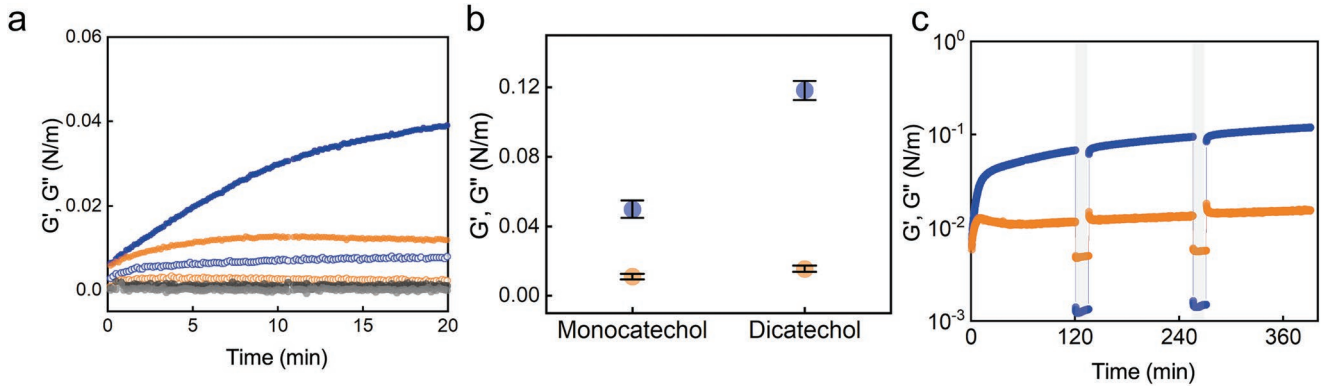

Figure 2. Interfacial rheology of ionically crosslinked surfactants. a) The storage (G′) (○) and loss moduli (G″) (○) of DC surfactants crosslinked with 2 mM Fe^{3+}, G′ (●) and G″ (●) of DC surfactants crosslinked with 20 mM Fe^{3+}, and G′ (●) and G″ (●) of the uncrosslinked counterparts. Measurements are done at 1 rad s^{-1} and 0.1% oscillation strain. b) G′ (●) and G″ (●) of MC and DC surfactants, crosslinked with Fe^{3+}, showing the increased robustness of membranes composed of DC surfactants after they have been in contact with Fe^{3+} ions for 4 h. c) Membranes are repetitively subjected to high (10%) (grey shaded area) and low (0.1%) strains (white area). The abrupt changes in G′ and G″ indicate that the membranes quickly recover after the stress has been released. Error bars represent the standard deviation of at least three repeats that have been measured on three independent samples.

the films to 10% for 15 min and monitoring the storage and loss moduli as a function of time. If strained to 10%, the loss modulus of the membrane is higher than the storage modulus, indicating that the membrane is broken and behaves like a liquid. Upon reduction of the strain to 0.1%, the membrane re-forms and G′ is again higher than G″, indicating that upon strain removal, the membrane quickly self-heals, as shown in Figure 2c. To assess whether our membranes would be self-healing at even higher strains, we perform a self-healing test by repetitively subjecting the membranes to even higher (100%) and low (0.1%) strains. Indeed, our membranes are self-healing even when subjected to a much higher strain differences, as shown in Figure S10, Supporting Information.

Our interfacial rheology results suggest the formation of thin membranes composed of ionically crosslinked dicatechol surfactants. If surfactants form a monolayer at the liquid-liquid interface, we expect the thickness of these membranes to be in the nanometer range. Small angle scattering (SAS) is a methodology that characterizes these lengths scales of materials in bulk.[35] Small angle neutron scattering (SANS) enables contrast matching between the aqueous core and the HFE7100 oil by adjusting the ratio between water (H_2O) and deuterium oxide (D_2O) in the core. If properly done, we do not see any scattering contrast between the core and the surrounding fluid such that all the observed scattering comes from the shell.[36] The diameter of the capsules is ≈100 µm, a value much larger than the maximum dimension of 300 nm that we can probe with SAS. At these high magnifications, the shell is observed as an infinite plane and can be modeled with a thin disk form factor P(q), as detailed in Figure S11, Supporting Information.[37] The scattering intensity $I(q)$ follows a power law decrease with q^{-2} within $0.03 < q < 0.12$ nm^{-1}, as shown in **Figure 3**a. This result is characteristic of 2D objects. A fit of this q-range reveals a dimension of about 11 nm, a value that agrees well with the expected shell thickness, which includes the surfactant tail, the catechol headgroups and the Fe^{3+} ions, but excludes any dimensions related to the core and surrounding solvent of the capsules, as shown in Figure 3a. To prove this matching, we replace the liquid in the core with pure water, as schematically shown in Figure 3b. SANS measurements reveal the scattering of a sharp interface in the same q-region, $0.03 < q < 0.12$ nm^{-1}, as observed by a q^{-4} power law decay of the scattered intensity. This decay reveals a typical Porod Behaviour of a net flat interface and indicates that the shell interface is dense and smooth.

Neutrons strongly interact with nuclei, such that the surfactants and Fe^{3+} present in the capsule shells contribute to the observed scattering. To clearly separate contributions of the two entities, we also probe our samples using X-rays that interact with electrons. If analyzed with small angle X-ray scattering (SAXS), capsules have an intrinsic contrast since Fe^{3+} scatters X-rays more efficiently than the other components of the system. The scattering curve of this sample displays a power law decay of q^{-2} within $0.17 < q < 0.60$ nm^{-1}, indicative of a 2D object, as shown in Figure 3a. However, compared to the SANS measurements, this decay occurs at higher q-ranges, relating to smaller dimensions. From fitting this q-range, we calculate a dimension of about 2 nm, which could be linked to the average size of Fe^{3+} clusters that from within the tris(hydroxymethyl) aminomethane (TRIS) buffer that we employ as aqueous solution. At $q < 0.09$ nm^{-1} and $q > 0.88$ nm^{-1}, the SAXS scattering curve exhibits the decay of q^{-4}, suggesting that the Fe^{3+} aggregates also form a compact shell with a smooth interface, and that they are not dispersed in the aqueous core. Hence, scattering results reveal a total shell thickness of about 11 nm that includes an ≈2 nm thick layer that primarily contains Fe^{3+} agglomerates. Subtracting this Fe^{3+}-rich layer from the overall shell thickness of 11 nm, we find an average thickness of the shell that mainly comprises the surfactant tails of 9 nm. This

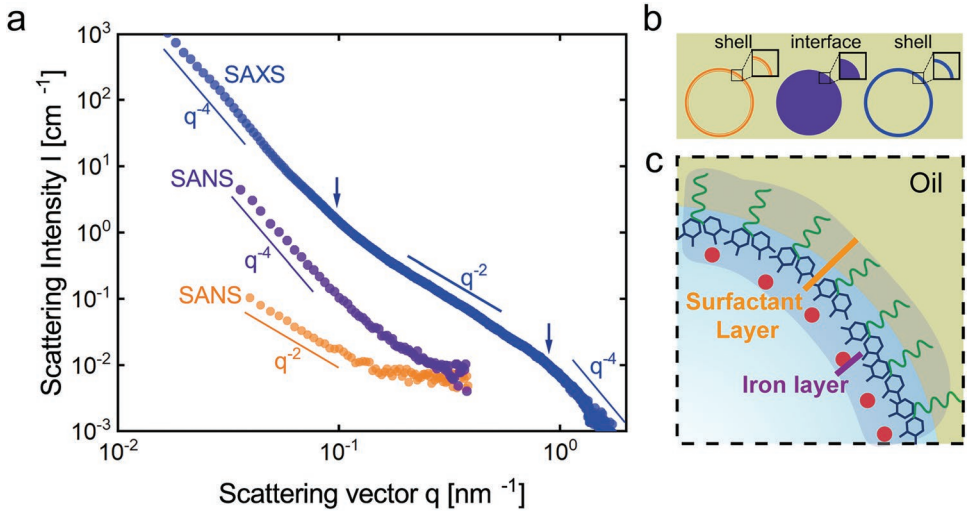

Figure 3. a) Small angle scattering of capsules produced by crosslinking the surfactant with Fe^{3+}: SANS measurements of capsules with zero contrast between core and solvent (orange) and those with aqueous cores dispersed in oil (violet). For capsules with aqueous cores, neutrons sense a sharp interface between the core and the solvent at $0.17 < q < 0.6$, observed by the q^{-4} decay. SAXS measurements of the capsules containing an aqueous core (blue). X-rays, that are mainly scattered by the Fe^{3+} layer, reveal a power law decay of q^{-2}, indicative of flat surfaces. b) Schematic illustration of the estimated length scales and expected contrast. Combined analysis of SAXS and SANS provides a total shell thickness of about 11 nm, and a Fe^{3+} layer thickness of about 2 nm.

ADVANCED MATERIALS INTERFACES
Open Access
www.advmatinterfaces.de

value is in good agreement with the theoretical estimation of 6 nm for the fully stretched length of the perfluorinated block and 3 nm for that of the J900 block, as calculated by adding bond lengths for the respective blocks and summarized in Figure 3c. These results support our hypothesis that the viscoelastic shell is composed of a single smooth compact monolayer of surfactants that are crosslinked with small Fe^{3+} clusters.

Our results demonstrate that difunctional block-copolymer surfactants can be converted into viscoelastic shells by crosslinking those located at the liquid-liquid interface with Fe^{3+}. We hence expect emulsion drops stabilized with such surfactants that are subsequently ionically crosslinked to be much more stable against coalescence than uncrosslinked counterparts. To test our expectation, we produce capsules from water-in-oil emulsions that are stabilized with the dicatechol surfactants. We ionically crosslink the surfactants by exposing them to a solution of $FeCl_3$ at pH 9. A solution of TRIS buffer is employed to increase the pH of the solution from acidic to basic: Fe^{3+} ions strongly bind to TRIS molecules, preventing the precipitation of iron oxide nanoparticles when the pH is increased above 3. Yet, because Fe^{3+} prefers binding to catechols over TRIS, we obtain a ligand exchange as soon as the Fe/TRIS solution is exposed to the functionalized surfactants, resulting in the formation of the viscoelastic shell.[38] Emulsion drops stabilized with polyethylene glycol (PEG) containing surfactants tend to coalesce if they are loaded with high concentrations of ions because salt partially collapses the PEG.[9] Indeed, drops that are stabilized with monocatechol functionalized surfactants, which are crosslinked with Fe^{3+}, coalesce if loaded with 50 mM sodium chloride. By contrast, drops stabilized with the dicatechol functionalized counterpart that is crosslinked with Fe^{3+} remain intact for at least 3 h even if loaded with 50 mM sodium chloride, as shown in the second row of **Figure 4**.

Surfactant-stabilized drops also tend to coalesce if exposed to elevated temperatures. For example, drops stabilized with the monocatechol functionalized surfactants that are crosslinked with Fe^{3+} coalesce at ≈50 °C even if they do not contain significant amounts of ions. By contrast, capsules composed of the ionically crosslinked dicatechol surfactant remain stable for at least 10 min if kept at 100 °C, as shown in the third row of Figure 4. To better visualize the mechanical robustness of the viscoelastic capsules, we deposit them onto a glass slide and deform them with a pipette tip that is pushed onto them. Even though they strongly deform such that their diameter increases 1.5-fold, they remain intact, in stark contrast to capsules composed of the monofunctional surfactant, as shown in the last row of Figure 4.

Our results reveal that capsules composed of the dicatechol functionalized surfactants, if crosslinked with Fe^{3+}, are stable even if exposed to salt concentrations up to 2 M, elevated temperatures, or mechanical stresses. However, because catechols only strongly interact with Fe^{3+} at pHs of 9 or above, these

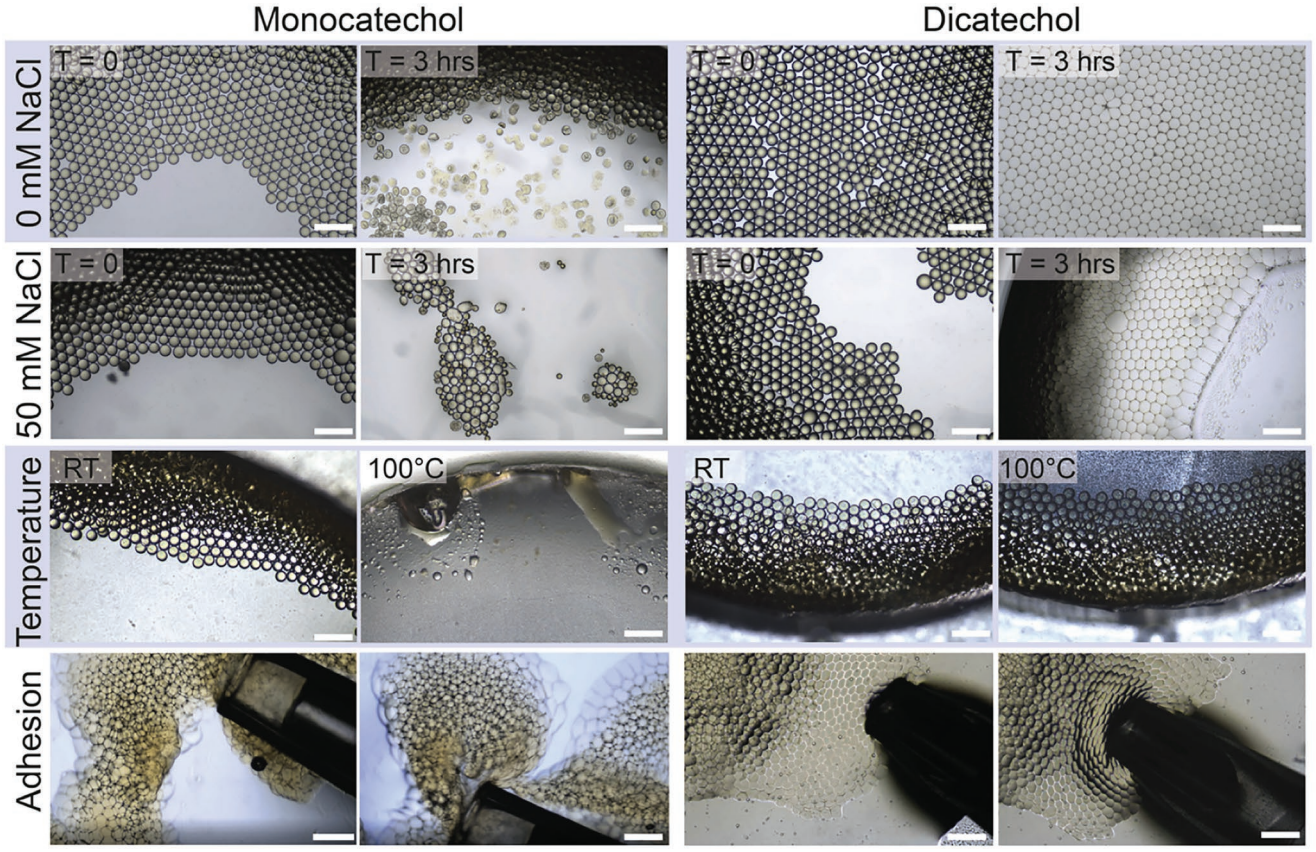

Figure 4. Stability of capsules produced by crosslinking MC or DC surfactants with 20 mM Fe^{3+} at pH 9. Capsules produced with DC surfactants are more stable when they are loaded with salt, heated to 100 °C, or mechanically stressed. Scale bar is 500 µm.

capsules can only be used under basic conditions, severely limiting their applicability especially for biomedical and food applications. To overcome this limitation, we functionalize the block-copolymer with a catechol derivative that has much lower pKa values such that it complexes Fe^{3+} even under physiologic conditions. A catechol derivative that has a pKa below 7 is nitrocatechol.[33] We therefore expect capsules composed of ionically crosslinked surfactants that have been functionalized with two nitrocatechols to be stable under physiologic pHs if crosslinked with Fe^{3+}. Indeed, capsules that are crosslinked through nitrocatechol-Fe^{3+} interactions are stable for at least 6 months at pH 7, which was the duration of our experiment. Hence, these capsules have the potential to be used for biomedical applications.

The mechanical properties of ionically crosslinked bulk hydrogels strongly depend on the chelator-ion interactions.[39] To test if this is also the case for our ionically crosslinked capsules, we crosslink dinitrocatechol functionalized surfactants with divalent ions. Unfortunately, these capsules break if crosslinked with divalent ions such as Cu^{2+}, as shown in Figure S12, Supporting Information. To expand the range of mechanical properties these capsules can attain, we synthesize a surfactant that is functionalized with two pyrogallols per molecule. Pyrogallols have three hydroxyl groups per benzene ring, as opposed to catechols and nitrocatechols that only have two of these groups. This additional hydroxy group enables crosslinking with di- and trivalent ions in bulk hydrogels.[33] To assess if this is also the case in 2D, we crosslink dipyrogallol functionalized surfactants with Fe^{3+}. Indeed, these capsules are stable for at least 6 months if crosslinked at pH 7. They also show remarkable stability if loaded with sodium chloride or heated up to 100 °C, similarly to what we observed for capsules formed from dinitrocatechol surfactants, as shown in Figure S13, Supporting Information. Interestingly, these surfactants can also be crosslinked with divalent ions. For example, if we crosslink them with Co^{2+}, they remain stable for at least 6 months at pH 7 and 9, as shown in Figure S14, Supporting Information. By contrast, if crosslinked with Ca^{2+}, capsules break as soon as they are produced. We assign this poor stability to the lack of a d-shell in Ca^{2+} and therefore its inability to form a coordination complex, as summarized in **Figure 5**. These results suggest that dipyrogallol stabilized surfactants can be crosslinked with any di- or trivalent ion that has d-shells even under physiologic conditions. This finding strongly facilitates the choice of crosslinking ions and broadens the range of mechanical properties that these thin viscoelastic membranes can attain.

We expect the capsule stability to scale with the density of surfactants at the capsule surface. To test this expectation, we quantify the packing density of surfactants functionalized with the three different chelators as a function of the crosslinking ions using a Langmuir trough, as shown in Figure S15, Supporting Information. Indeed, the stability of the capsules, measured as the time the drops remain stable if kept at room temperature, increases as the mean molecular area decreases, as summarized in **Figure 6**a. The drop stability often scales with the interfacial tension. To test if we observe a similar trend for the stability of our capsules, we quantify the interfacial tension between the water and the oil containing 1 wt% of the surfactants functionalized with the three different chelators as a

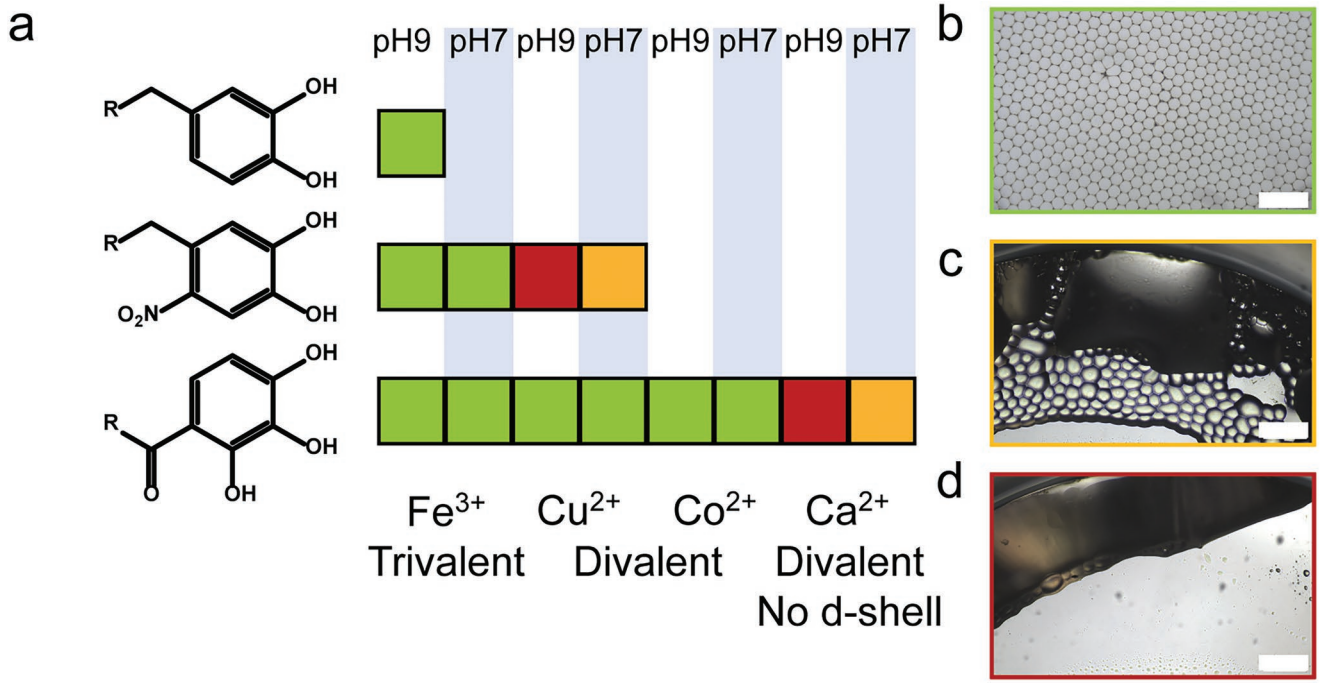

Figure 5. a) Molecular structures of catechol (top), nitrocatechol (middle), and pyrogallol (bottom). Capsules produced from surfactants functionalized with two of the corresponding chelators per molecule that have been crosslinked with different ions under neutral and basic pHs. Capsules that are stable for at least 6 months are shown in green (■), those that are stable up to 30 min in yellow (■), and those that coalesce immediately are shown in red (■). Digallol functionalized surfactants can be crosslinked with divalent and trivalent ions at neutral and basic pHs. Microscope images of b) stable capsules (DG/Fe^{3+} pH 9), c) capsules stable up to 30 min (DG/Ca^{2+} pH 7) and d) unstable capsules taken 5 min after assembly (DNC/Cu^{2+} pH 9). Scale bars are 750 µm.

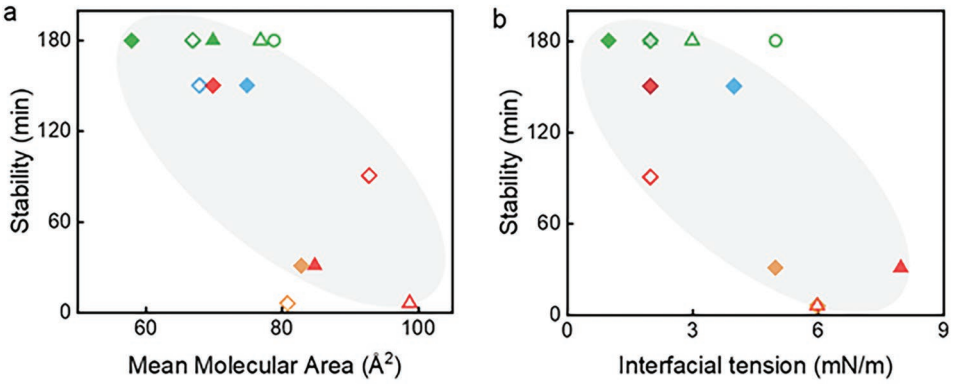

Figure 6. Influence of the a) mean molecular area and b) interfacial tension on the capsule stability measured as the time capsules remain stable if kept at room temperature. Results are shown for DC (●), DNC (▲) and DG (◆) that are crosslinked with Fe^{3+} (■), Co^{2+} (■), Cu^{2+} (■), Ca^{2+} (■), and in their uncrosslinked state (■) at pHs 7 (filled symbols) and 9 (empty symbols).

function of the crosslinking ion. Indeed, the lower the interfacial tension, the higher is the capsule stability, as summarized in Figure 6b. To assess the sample-to-sample variability, we perform these experiments on at least three independent samples. Because of the relatively large difference between the different time points we measured, we did not observe any sample-to-sample variability in this measurement such that, given the nature of the experiment, the error bars are zero.

Because the stability of the capsules scales with the mean molecular area and the interfacial tension, we expect the two latter parameters to also be correlated. Indeed, the interfacial tension linearly scales with the mean molecular area of the surfactant, as shown in **Figure 7**a and detailed in Figure S16, Supporting Information. Hence, by choosing the appropriate the ion-chelator pair, we can tune the packing density of the surfactants and hence the stability of the capsules. To quantify the capsule stability more rigorously, we assess the rheological properties of the membranes in 2D. We perform interfacial rheology measurements on membranes composed of the three different types of surfactants that are crosslinked with di- and trivalent ions, respectively, as shown in Figure S18 and Table S1, Supporting Information. Indeed, the storage modulus linearly increases with increasing surfactant packing density, as summarized in Figure 7b. Hence, by tuning the chelator-ion pair, we cannot only tune the dissipation times of the crosslinks and hence, the viscoelastic properties of the shell, but also its stiffness. Due to the high reproducibility of interfacial rheology experiments that we tested on one data point, as shown in Figure S19, Supporting Information, the large sample volumes required for this technique, and in agreement with what is typically done within this community,[40–42] the values in Figure 7b have only been measured once.

A key parameter that determines the usefulness of capsules is the ability to change their permeability in situ. We expect the permeability of surfactants to be much lower if we ionically crosslink them as we form a viscoelastic shell that is less dynamic than uncrosslinked surfactants self-assembled at liquid-liquid interfaces. To test our expectation, we fabricate capsules composed of surfactants functionalized with different chelators and crosslink them with Fe^{3+}. To encapsulate hydrophilic reagents while being able to disperse the capsules in aqueous media, we produce them from water-oil-water double emulsion templates. Double emulsions are composed of an aqueous core containing fluorescein and 15 wt% PEG, a middle phase composed of HFE7500 containing 1 wt% of the surfactant and outer aqueous phase containing 10 wt% polyvinyl alcohol

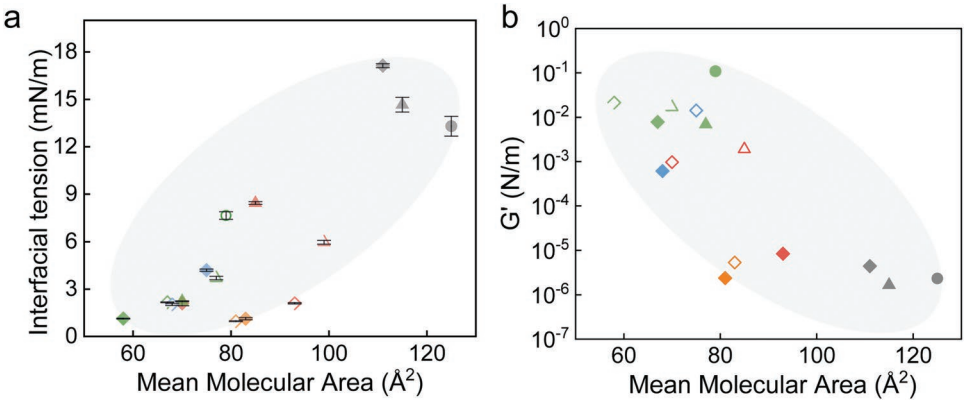

Figure 7. Influence of mean molecular area on a) interfacial tension and b) storage modulus G′ for DC (●), DNC (▲) and DG (◆) surfactants that are crosslinked with Fe^{3+} (■), Co^{2+} (■), Cu^{2+} (■), Ca^{2+} (■), and in their uncrosslinked state (■) at pHs 7 (filled symbols) and 9 (empty symbols). Error bars represent the standard deviation of at least three repeats that have been measured on three independent samples.

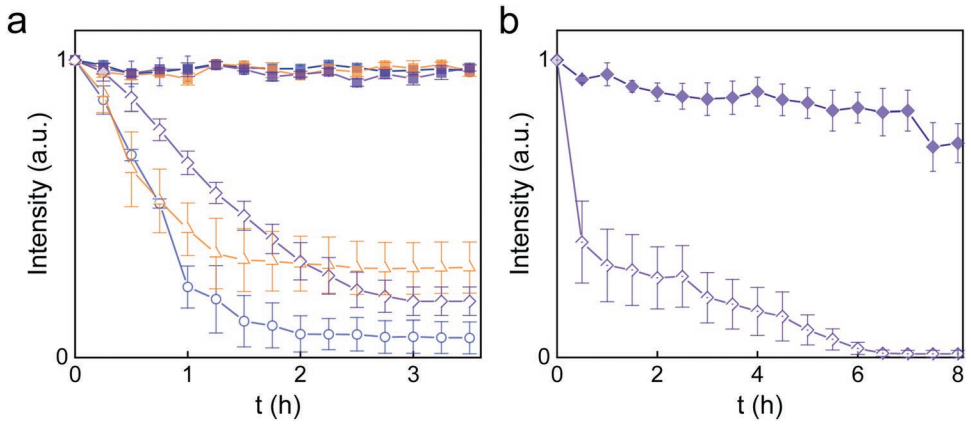

Figure 8. Fluorescent intensity of a) the aqueous core of capsules composed of surfactants that have been functionalized with DC (●), DNC (▲), and DG (◆) surfactants before they were crosslinked with Fe^{3+} at pH 9. Upon addition of EDTA, most Fe^{3+} ions are scavenged from the shell such that the majority of the surfactants is not ionically crosslinked anymore. As a result of this de-crosslinking, the capsule permeability strongly increases, as shown by the empty symbols. b) Fluorescent intensity of the aqueous core of capsules composed of DG functionalized surfactants with an inner phase composed of cell culture media base buffer DMEM. Even if the core of capsules is composed of DMEM, they efficiently retain fluorescein if crosslinked with Fe^{3+} (◆), in stark contrast to the non-crosslinked counterparts (◇). Error bars represent the standard deviation of at least three repeats that have been measured on three independent samples.

(PVA), 20 mM Fe^{3+} and 0.1 M TRIS base. Indeed, no measurable amount of fluorescein is released from any of the tested ionically crosslinked shells within 3 h, as shown in **Figure 8**a. To trigger the release of the fluorescein, we add ethylenediaminetetraacetic acid (EDTA), a molecule that scavenges Fe^{3+} ions from the shell as these ions have a higher affinity to EDTA than to any of the tested chelators. Indeed, the resulting defective capsules are much more permeable: at least 50% of the fluorescein is released within 60 min, as shown in Figure 8a. These results demonstrate the power of the ionic crosslinking to minimize the permeability of shells and maximize their mechanical stability while maintaining the fluidity of the shell required to rapidly self-heal if the capsules become defective. Our results indicate that all these parameters are closely related to each other and can conveniently be tuned by the choice of the chelator-ion pair.

To demonstrate the potential of our capsules for drop-based high throughput screening tests and cell studies, we replace the aqueous core of the double emulsions with a cell culture media base buffer, namely Dulbecco's Modified Eagle Medium (DMEM 1X). To ionically crosslink the surfactants, we add 20 mM Fe^{3+} to the outer phase. To assess the permeability, we also include 0.01 wt% fluorescein in the core. Indeed, even if the core of these capsules is composed of DMEM, they efficiently retain encapsulants as small as 340 Da for at least 8 h, which is the duration of our experiment, as shown in Figure 8b. By contrast, counterparts whose shell has not been ionically crosslinked release 70% of fluorescein within 60 min, as shown in Figure 8b. Importantly such capsules can also be formed from water in oil single emulsion drops that can be produced at much larger scales, as previously reported in the literature.[22,43–44] Upon ionic crosslinking, the capsules can be transferred into aqueous solutions without compromising their stability, as illustrated in Figure S20, Supporting Information. These results demonstrate the potential of our capsules for biomedical applications and drop-based single cell studies.

3. Conclusion

Surfactants functionalized with two chelators per molecule can be converted into well-defined viscoelastic shells with a thickness of order 10 nm upon crosslinking with an appropriate ion. The stability and permeability of the resulting capsules scale with the interfacial tension and packing density of the surfactants at the liquid-liquid interface and the storage modulus of the viscoelastic membrane that forms after ionic crosslinking of the surfactants. These parameters can be closely tuned by the choice of the chelator-ion pairs. The key requirement for an efficient ionic crosslinking is the presence of a d-shell within the crosslinking ions. The wide choice of crosslinking ions enables tuning the mechanical properties and permeability of these capsules over a wide range. The reversible ion-chelator bonds enable capsules to rapidly self-heal if defective, thereby increasing their robustness. Importantly, we employ chelators with pKa values at or below 7, such that capsules are stable under physiologic conditions. These capsules thus have the potential to be used, for example, in in vitro cell studies as individually dispersed entities containing cells or other reagents such as nutrients. With additional work devoted to replacing the perfluorinated block of the surfactant with a hydrocarbon-based one, we envisage these surfactants to become biocompatible or even food grade. We foresee the resulting next generation of viscoelastic capsules to also be used, for example, for pharmaceutical or even food applications.

4. Experimental Section

Surfactant Synthesis: All chemicals, namely 3-(3,4,-dihydroxyphenyl) propionic acid (hydrocaffeic acid, HA) (Abcr, Germany), *N*-hydroxysuccinimide (NHS) (TCI Chemicals), *N,N*-dicyclohexylcarbodiimide (DCC), anhydrous ethyl acetate anhydrous *N,N*-Dimethylformamide (DMF), pyridine, *N,N,N′,N′*-Tetramethylethylenediamine (TEMED), α-α-α-trifluorotoluene (TFT), dichloromethane (DCM), methanol (MeOH), gallic acid (GA),

Celite S, magnesium sulphate and 1,3-diaminopropan-2-ol (Sigma-Aldrich), *p*-toluene- sulfonyl chloride and boron tribromide (Acros Organics), Jeffamine ED900 (J900) (Mw 900 g mol^{-1}, Huntsman), fluorinated block of the surfactants FSH (Krytox 157 FSH, Chemours, USA), fluorinated oil HFE-7100 (3 M, USA), thionyl chloride (Merck), 3,4-dimethoxy-6-nitrocinnamic acid (Fluorochem) were used as received.

DC Synthesis: 1 mol of HA and 1 mol of NHS were added to 30 mL dry ethyl acetate. Separately, 1 mol DCC was added to 10 mL dry ethyl acetate. The DCC solution was added to a stirring solution of HA/NHS. This reaction was carried out at room temperature and overnight under argon. The resultant solution was filtered, and collected, while the retained precipitates were discarded. Based on a 95% yield, 0.5 mol equivalent 1,3-diaminopropan-2-ol was dissolved separately in 10 mL of dry ethyl acetate and the solution was added to the NHS-HA solution. This reaction was carried out at room temperature and overnight under argon. The resultant solution was dried under rotary vacuum (Hei-VAP, Heidolph, Germany) at 1 mbar, 40 °C for 2 h to obtain the di-hydrocaffeic acid di-amide alcohol product, as shown in Figure S13, Supporting Information. 1 mol of the di-amide alcohol was dissolved in DMF at 0 °C to which 1.2 mol eq. of pyridine and 1.2 mol of p-toluene-sulfonyl chloride were added. The reaction mixture was stirred over night at room temperature.[45] The solvent was removed under reduced pressure at 1 mbar, 40 °C for 2 h. The tosylate was added to DMF, 1.2 mol eq. of Jeffamine ED-900 (J900) was dissolved separately in DMF. J900 solution was added to the R-OTs solution. 1.2 eq. of TEMED were added to drive the reaction forward. This reaction was carried out at room temperature and overnight under argon. Resultant solution was dried under rotary vacuum at 1 mbar and 50 °C for 2 h. The dried product is the Dicatechol-J900. 0.63 mmol FSH was dissolved in dry HFE-7100 and argon was bubbled into the solution for 15 min. 10 mol equivalent thionyl chloride was added to the FSH solution and refluxed for 5 h at 65 °C under an argon blanket. Separately, 1.1 mol equivalent of the dicatechol-J900 was dehydrated in trifluorotoluene (TFT) at 90 °C under vacuum for 30 min. Finally, the dried dicatechol-J900 was solubilized in 20 mL anhydrous dichloromethane. After the reaction between FSH and thionyl chloride, the resultant solution was dehydrated at 90 °C under vacuum for 30 min. Finally, the dried activated FSH was dissolved in 15 mL dry HFE 7100. For the reaction between dicatechol-J900 and FSH, the dicatechol-J900 solution was added to the activated FSH under argon. To minimize the risk of potential byproducts, such as Jeffamine900 that is functionalized with Krytox at both ends, 1.1 mol equivalents of the catechol-containing intermediate were added. Thereby, the chance of having bi-catechol functionalized Jeffamine was increased. This side-product can readily be removed during the last purification step as it is insoluble in HFE7100, where the final product was extracted in a mixture of methanol/HFE7100. The reaction was carried out by refluxing at 65 °C under an argon blanket overnight. The resultant solution was cooled to room temperature. 10 mL of HFE 7100 was added to dissolve the products. 90 mL of methanol was added to the product solution and mixed. Precipitates (products) were separated by centrifugation (3000 g, 3 °C, 15 min) (Mega Star, 1.6R, VWR) and the supernatant solution was removed. This washing step was repeated three times. The leaned product was dried under rotary vacuum at 1 mbar and 50 °C for 30 min. Products were freeze dried overnight (FreeZone 2.5, Labconco, USA). The resulting products appeared as an off-white gel, as shown in Figure S6, Supporting Information. The whole reaction pathway can be found in Figure S7, Supporting Information.

DNC Synthesis: The same procedure as for the DC synthesis was followed but hydrocaffeic acid was replaced with nitrocatechol, which was synthesized as follows: To a suspension of 1 g of 3,4-dimethoxy-6-nitrocinnamic acid in 50 mL DCM were added dropwise at RT under a nitrogen atmosphere 20 mmol eq. of boron tribromide. The mixture was stirred overnight. To the cooled solution, 200 mL of water were added. After 1 h of hydrolysis, the organic layer was separated, and the aqueous layer extracted with ethyl acetate (5 × 50 mL). The organic layers were collected and refluxed with charcoal for 30 min. The suspension was filtered over Celite S twice and dried over $MgSO_4$. Solvent was removed under reduced pressure. NMR spectrum of (2E,2″E)-*N*,*N*″-(2-hydroxypropane-1,3-diyl)bis(3-(4,5-dihydroxy-2-nitrophenyl)acrylamide) can be found in Figure S3, Supporting Information, and the full molecular structure in Figure S8, Supporting Information.

DG Synthesis: The same procedure as for the DC synthesis was followed but hydrocaffeic acid was replaced with gallic acid. NMR spectrum of *N*,*N*′-(2-hydroxypropane-1,3-diyl)bis(3,4,5-trihydroxybenzamide) can be found in Figure S4, Supporting Information, and the full molecular structure in Figure S9, Supporting Information.

Interfacial Rheology: Interfacial rheology experiments were performed using a DHR-3 TA Instruments rheometer, with a Double-Wall Ring (DWR) geometry. The oil/water interface was found by performing an axial measurement before every experiment. Oscillation sweeps were made at room temperature using a frequency of 1 rad s^{-1}. Frequency sweep measurements were made at room temperature using a 0.1% strain.[46] Time sweep measurements for storage modulus (G′) comparisons were made at room temperature, using a 0.1% strain and 1 rad s^{-1} frequency. Self-healing tests were performed by cycling time sweeps at 0.1% strain and 1 rad s^{-1} frequency (where the membrane is intact) with time sweeps at 100% strain and 1 rad s^{-1} frequency (where the membrane is broken). Storage moduli of all ion-chelator pairs were reported after 4 h, for comparison.

Small Angle Neutron Scattering: Experiments were performed at the Swiss Spallation Neutron Source, SINQ, Paul Scherrer Institut using the SANS-I instrument. The neutron wavelength was set to 6 Å. A sample-to-detector distance of 18 m attained the low range of scattering vectors q. The capsules were measured in quartz cuvettes with a thickness of 1 mm. The absolute intensity was corrected for incoherent scattering of water, sample thickness, and transmission. The sample for SANS with contrast matching was prepared using a ratio of 50.5/49.5 wt% of H_2O/D_2O for the aqueous core, while the core of the second sample was composed mainly of water.

Small-Angle X-ray Scattering: Measurements were performed at the Swiss Light Source, cSAXS, Paul Scherrer Institute, at a wavelength of 1 Å and detector distance of 7.1065 m. The X-ray beam was focused on the detector to 50 × 25 μm^2 onto borosilicate glass capillaries with a 1 mm diameter. Ten positions were measured along the capillary with exposure times of 0.1 s followed by a pause of 0.1 s. These patterns were monitored for radiation damage and finally averaged to improve the statistics.

Fabrication of Microfluidic Device: All microfluidic masks were made using soft lithography.[47] The microfluidic devices were produced by mixing 10:1 PDMS to curing agent (Dow Corning, USA) and cured overnight. For the single emulsions, the channels were made fluorophilic by injecting a HFE-7100-based solution containing 2% trichloro(1H,1H,2H,2H-perfluorooctyl)silane (Sigma-Aldrich, USA) in all the channels for 10 min, before drying them with compressed air. The first junction of double emulsion devices was made fluorophilic by treating it with the same solution as above, while the second junction was made hydrophilic by treating it with an aqueous solution containing 2% polydiallyldimethylammonium chloride (Sigma-Aldrich, USA). The solutions were left in the channels for 10 min before drying the devices with compressed air.

Production of Emulsions: Emulsion drops were produced with a microfluidic flow focusing device. Single emulsions were produced by injecting the outer phase at 3000 µL h^{-1} using a syringe pump (Cronus Sigma 1000, Labhut, UK). The inner phase was injected at 1000 µL h^{-1}. Double emulsions were produced by injecting an inner aqueous phase containing 15 wt% PEG 6000 Da (Sigma Aldrich) and 0.01 wt% fluorescein disodium salt (ABCR Chemicals), either in deionized water, for permeability triggering, or in Dulbecco's Modified Eagle Medium (DMEM 1X), to assess the potential of these capsules in the biomedical field. The middle oil phase was composed of HFE-7100 containing 1 wt% surfactant, while the outer aqueous phase contained 10 wt% partially hydrolyzed polyvinyl alcohol (PVA) 13–18 kDa (Sigma-Aldrich, USA), 20 mM Fe^{3+} and 0.1 M TRIS base (Sigma Aldrich). The flow

rates for the inner, middle, and outer phases were 1000, 1200, and 5000 µL h^{-1}, respectively.[48] To avoid osmotic pressure imbalance, all aqueous solutions used to make double emulsions were osmotically balanced with the aid of an osmometer (Advanced Instruments, Fiske 210).

Pendant Drop Measurements: All the interfacial tension values were measured using the pendant drop method. A sample of each solution was inserted in a 1 mL syringe and loaded onto a Krüss DSA 30 drop shape analyzer. The drops were created and analyzed using the Krüss Advance software (v.1.6.2.0).

Langmuir Trough Measurements: The mean molecular area of the surfactants adsorbed on the air-water interface was determined with a Langmuir trough (KN2002, KSV Nima, Biolin Scientific, Finland). It was approximated to be similar to that at the oil-water interface. Different aqueous solutions (with or without ions at pHs 7 and 9) were employed. To measure the surface pressure, a paper Wilhelmy plate was used. To test if the trough and the Wilhelmy plate were clean, it was made sure the surface pressure stayed below 0.3 mN m^{-1} when closing the barriers without adding any surfactant. 0.1 wt% of the surfactant was dissolved in Novec HFE-7100 and 75 µL of this solution was slowly added to the water–air interface. To ensure all the HFE-7100 was evaporated, the authors had waited for 8 h before the experiments were performed by closing the barriers at a speed of 5 mm min^{-1}. The area where the slope of the surface pressure against the mean molecular area sharply increases for the first time was assigned to the minimum area the surfactant occupies.

Quantification of Fluorescence Intensity: 1 µL of double emulsions was added to 1.5 mL of an osmotically balanced aqueous solution, and emulsions were imaged every 15 min using a fluorescent microscope (Eclipse Ti-S, Nikon). The fluorescence images were analyzed using a custom-made MATLAB code that quantifies the evolution of the fluorescent intensity of double emulsion cores over time.

Supporting Information

Supporting Information is available from the Wiley Online Library or from the author.

Acknowledgements

The authors would like to thank all the members of the Soft Materials Laboratory (SMaL), in particular Chuen-Ru Li for sharing the TRIS-iron protocol and Alexandra Thoma for the help with double emulsions. They would also like to thank Richard Blackall and Dr. Mathias Steinacher for fruitful discussions, and Dr. Enzo Bomal for the help with interfacial rheology experiments. The authors acknowledge the time for measurements during proposal 20210413 granted to PSI/SLS/cSAXS and proposal 20210940 granted to PSI/SINQ/SANS-I. The authors thank Ana Diaz for her support during the cSAXS beamtime, and Fabrice Cousin for the discussions about the scattering data analysis. The work was financially supported by Swiss National Science Foundation through the bio-inspired material NCCR (205603).

Conflict of Interest

The authors declare no conflict of interest.

Data Availability Statement

The data that support the findings of this study are available from the corresponding author upon reasonable request.

Keywords

capsule stability, catechols, interfacial rheology, viscoelastic capsules

Received: December 13, 2022
Revised: February 15, 2023
Published online: April 4, 2023

[1] L. J. De Cock, S. De Koker, B. G. De Geest, J. Grooten, C. Vervaet, J. P. Remon, G. B. Sukhorukov, M. N. Antipina, *Angew. Chem., Int. Ed.* **2010**, *49*, 6954.
[2] M. A. Augustin, Y. Hemar, *Chem. Soc. Rev.* **2009**, *38*, 902
[3] I. M. Martins, M. F. Barreiro, M. Coelho, A. E. Rodrigues, *Chem. Eng. J.* **2014**, *245*, 191,
[4] X. Zhou, S. Yamashita, M. Kubota, H. Kita, *ACS Omega* **2022**, *7*, 5442
[5] W. H. Gunzburg, M. M. Aung, P. Toa, S. Ng, E. Read, W. J. Tan, E. V. Brandtner, J. Dangerfield, B. Salmons, *Microb. Cell Fact.* **2020**, *19*, 216.
[6] A. J. Svagan, C. B. Koch, M. S. Hedenqvist, F. Nilsson, G. Glasser, S. Baluschev, M. L. Andersen, *Carbohydr. Polym.* **2016**, *136*, 292.
[7] M. Yan, J. Du, Z. Gu, M. Liang, Y. Hu, W. Zhang, S. Priceman, L. Wu, Z. H. Zhou, Z. Liu, T. Segura, Y. Tang, Y. Lu, *Nat. Nanotechnol.* **2010**, *5*, 48.
[8] P. Gruner, B. Riechers, B. Semin, J. Lim, A. Johnston, K. Short, J.-C. Baret, *Nat. Commun.* **2016**, *7*, 10392.
[9] N. Ataci, A. Sarac, *Am. J. Analyt. Chem.* **2014**, *5*, 22.
[10] G. Etienne, A. Vian, M. Biocanin, B. Deplancke, E. Amstad, *Lab Chip* **2018**, *18*, 3903.
[11] A. Abbaspourrad, S. S. Datta, D. A. Weitz, *Langmuir* **2013**, *29*, 12697.
[12] C. J. Ochs, G. K. Such, Y. Yan, M. P. van Koeverden, F. Caruso, *ACS Nano* **2010**, *4*, 1653.
[13] A. Vian, E. Amstad, *Soft Matter* **2019**, *15*, 1290.
[14] A. Abbaspourrad, N. J. Carroll, S. H. Kim, D. A. Weitz, *J. Am. Chem. Soc.* **2013**, *135*, 7744
[15] D. B. Flies, L. Chen, *J. Immunol. Methods* **2003**, *276*, 239,
[16] S. Mohammad, M. Modarres-Gheisari, R. Gavagsaz-Ghoachani, M. Malaki, P. Safarpour, M. Zandi, *Ultrason. Sonochem.* **2019**, *52*, 88.
[17] M. Karg, A. Pich, T. Hellweg, T. Hoare, L. A. Lyon, J. J. Crassous, D. Suzuki, R. A. Gumerov, S. Schneider, I. I. Potemkin, W. Richtering, *Langmuir* **2019**, *35*, 6231.
[18] N. Aryanti, R. A. Williams, *MATEC Web Conf.* **2018**, *156*, 08001
[19] S. J. Shepherd, C. C. Warzecha, S. Yadavali, R. El-Mayta, M. G. Alameh, L. Wang, D. Weissman, J. M. Wilson, D. Issadore, M. J. Mitchell, *Nano Lett.* **2021**, *21*, 5671.
[20] E. Amstad, M. Chemama, M. Eggersdorfer, L. R. Arriaga, M. P. Brenner, D. A. Weitz, *Lab Chip* **2016**, *16*, 4163.
[21] S. Yadavali, D. Lee, D. Issadore, *Sci. Rep.* **2019**, *9*, 12213.
[22] M. Steinacher, E. Amstad, *ACS Appl. Mater. Interfaces* **2022**, *14*, 13952.
[23] J. Du, S. P. Armes, *J. Am. Chem. Soc.* **2005**, *127*, 12800.
[24] A. C. Bijlard, S. Winzen, K. Itoh, K. Landfester, A. Taden, *ACS Macro Lett.* **2014**, *3*, 1165.
[25] M. Summers, J. Eastoe, R. K. Heenan, D. Steytler, *J. Dispers. Sci. Technol.* **2001**, *22*, 597.
[26] W. Zhang, R. Wang, Z. Sun, X. Zhu, Q. Zhao, T. Zhang, A. Cholewinski, F. K. Yang, B. Zhao, R. Pinnaratip, P. K. Forooshani, B. P. Lee, *Chem. Soc. Rev.* **2020**, *49*, 433.
[27] S. A. Cazzell, B. Duncan, R. Kingsborough, N. Holten-Andersen, *Adv. Funct. Mater.* **2021**, *31*, 2009118.
[28] E. Faure, C. Falentin-Daudré, C. Jérôme, J. Lyskawa, D. Fournier, P. Woisel, C. Detrembleur, *Prog. Polym. Sci.* **2013**, *38*, 236.

[29] N. Holten-Andersen, M. J. Harrington, H. Birkedal, P. B. Messersmith, K. Y. C. Lee, J. H. Waite, *Proc. Natl. Acad. Sci. USA* **2011**, *109*, 2651.
[30] J. H. Ryu, Y. Lee, W. H. Kong, T. G. Kim, T. G. Park, H. Lee, *Biomacromolecules* **2011**, *12*, 2653.
[31] M. Shin, K. H. Song, J. C. Burrell, D. K. Cullen, J. A. Burdick, *Adv. Sci.* **2019**, *6*, 1901229.
[32] G. Etienne, I. L. H. Ong, E. Amstad, *Adv. Mater.* **2019**, *31*, 1808233.
[33] A. Charlet, V. Lutz-Bueno, R. Mezzenga, E. Amstad, *Nanoscale* **2021**, *13*, 4073.
[34] P. Wilde, A. Mackie, F. Husband, P. Gunning, V. Morris, *Adv. Colloid Interface Sci.* **2004**, *108–109*, 63.
[35] J. P. Cotton, In *Neutron, X-ray and Light Scattering*, (Eds.: P. Lindner, T. Zemb), North Holland, New York **1991**.
[36] J. Jestin, S. Simon, L. Zupancic, L. Barre, *Langmuir* **2007**, *23*, 10471.
[37] F. Cherhal, F. Cousin, I. Capron, *Biomacromolecules* **2016**, *17*, 496.
[38] S. B. Gupta, T. Mohamed, M. Lee, *J. Solution Chem.* **2013**, *42*, 2296.
[39] S. Kim, A. U. Regitsky, J. Song, J. Ilavsky, G. H. McKinley, N. Holten-Andersen, *Nat. Commun.* **2021**, *12*, 667.
[40] E. Hermans, S. M. Bhamla, P. Kao, G. G. Fuller, J. Vermant, *Soft Matter* **2015**, *11*, 8048.
[41] S. Reynaert, P. Moldenaers, J. Vermant, *Phys. Chem. Chem. Phys.* **2007**, *9*, 6463
[42] B. Madivala, S. Vandebril, J. Fransaer, J. Vermant, *Soft Matter* **2009**, *5*, 1717.
[43] Z. Chen, Y. Zhao, Y. Zhao, H. Thomas, X. Zhu, M. Moller, *Langmuir* **2018**, *34*, 10397.
[44] M. Steinacher, A. Cont, H. Du, A. Persat, E. Amstad, *ACS Appl. Mater. Interfaces* **2021**, *13*, 15601.
[45] R. Scanga, L. Chrastecka, R. Mohammad, A. Meadows, P. L. Quan, E. Brouzes, *RSC Adv.* **2018**, *8*, 12960.
[46] R. Van Hooghten, V. E. Blair, A. Vananroye, A. B. Schofield, J. Vermant, J. H. J. Thijssen, *Langmuir* **2017**, *33*, 4107.
[47] L. R. Arriaga, S. S. Datta, S. Kim, E. Amstad, T. E. Kodger, F. Monroy, D. A. Weitz, *Biophys. J.* **2014**, *106*, 42a.
[48] I. L. H. Ong, E. Amstad, *Small* **2019**, *15*, 1903054.